Closed-Form Solutions for Arbitrary Laminated Anisotropic Cylindrical Shells (Tubes) Including Shear Deformation

Reaz A. Chaudhuri* and Kamal R. Abu-Arja†
University of Utah, Salt Lake City, Utah

Heretofore unavailable closed-form solutions are presented for arbitrarily laminated anisotropic cylindrical shells subjected to axially varying internal pressure. These solutions are obtained under the framework of the constant-shear-angle theory (CST) or the first-order shear-deformation theory (FSDT) for arbitrary boundary conditions. A unified CST-based shell theory, which is an extension of Love's first approximation theory or Love-Kirchhoff hypothesis, with four popular kinematic relations as special cases, has been employed into the formulation. The previously obtained CST-based solutions for symmetric/unsymmetric cross-ply and balanced-unsymmetric/unbalanced-symmetric angle-ply cylindrical shells under the same loading conditions have been shown to be special cases of the present solution. The available solution based on the classical lamination theory (CLT) can be obtained from the present solution in the limiting case of the transverse shear rigidities approaching infinity. Numerical results have been presented for two-layer thick cylindrical shells (tubes) with SS1-type simply supported boundary conditions and have been compared with the corresponding CLT-based closed-form solutions and also the finite-element solutions based on the layerwise constant-shear-angle theory (LCST). These are expected to serve as benchmark solutions for future comparisons and to facilitate the employment of asymmetric lamination in design, known as composite tailoring.

Nomenclature

A_{ij},B_{ij},D_{ij} = extensional, coupling, and bending rigidities, respectively, for $i, j = 1, 2, 6$
A_{ij} = transverse shear rigidities (including coupling) for $i,j = 4,5$
L = length of the circular cylindrical shell
$M_x,M_\theta,M_{x\theta},M_{\theta x}$ = bending and twisting moments per unit length
$N_x,N_\theta,N_{x\theta},N_{\theta x}$ = surface-parallel normal and shear-stress resultants per unit length
$\pm p(x)$ = axially varying (axisymmetric) pressure loading per unit area of the middle surface (+, internal; −, external)
$\pm p_0$ = uniform pressure (+, internal; −, external)
Q_x,Q_θ = transverse shear-stress resultants per unit length
R = radius of the reference (middle) surface of the cylindrical shell
t = thickness of the laminated shell
u_0,v_0 = surface-parallel displacement components at the reference surface in the axial and hoop directions, respectively
w = transverse or radial displacement component
x,θ,z = right-hand cylindrical shell coordinates
$\epsilon_1,\epsilon_2,\gamma_{12}$ = surface-parallel normal and shearing strains at a point
$\epsilon_1^0,\epsilon_2^0,\gamma_{12}^0$ = surface-parallel normal and shearing strains at the reference (middle) surface
$\bar{\theta}$ = fiber orientation angle of the outer layer
$\kappa_1,\kappa_2,\kappa_{12}$ = changes of curvature and twist
$\nu_{12},\nu_{13},\nu_{23}$ = major Poisson's ratios of an orthotropic lamina
$\sigma_x,\sigma_\theta,\tau_{x\theta}$ = surface-parallel normal and shearing stresses

Received Sept. 28, 1987; revision received Aug. 22, 1988.

*Assistant Professor, Department of Civil Engineering. Member AIAA.
†Postdoctoral Research Fellow.

Introduction

THE advent of fiber-reinforced composite materials, often used in the form of laminated shells in aerospace, hydrospace, and ground-based structural applications, has been hailed as "the biggest technical revolution since the jet engine."[1] This is because they possess such beneficial properties as high strength-to-weight and stiffness-to-weight ratios, fatigue life, corrosion resistance, and so forth.[2] These materials offer, for the first time, the possibility of optimum design of such structures as rocket motor cases, through the variation of fiber orientation, stacking pattern, and choice of fiber and matrix materials. However, this process, known as composite tailoring, is not without its price, because it introduces into the analysis such complexities as the anisotropy of the individual laminae and asymmetry of lamination, in general, that result in various coupling effects, first noted by Ambartsumyan,[3] who considered orthotropic layers.

Most of the analyses of the fiber-reinforced laminated shells employ the classical lamination theory (CLT), based on the Love-Kirchhoff hypothesis (also known as Love's first approximation theory), which ignores the transverse shear deformation. Among these, studies by Dong et al.,[4] Reuter,[5] Bert and Reddy,[6] and Chaudhuri et al.[7] are worth mentioning. Recently, Abu-Arja and Chaudhuri[8,9] have presented closed-form solutions of complete cross-ply and angle-ply cylindrical shells under internal pressure, based on the constant shear-angle theory (CST), also known as first-order shear deformation theory (FSDT), of which Reuter's[5] solutions, based on the CLT and Donnell's[10] kinematic relations, become special cases. Although the closed-form solutions on cross-ply and

angle-ply cylindrical shells offer the opportunity to develop a fundamental understanding of the complex deformation behavior of fiber-reinforced laminated shells, these studies do not appear to be that useful to the practical designers of laminated shell structures, e.g., rocket motor cases, wherein various combinations of these layups are usually employed. The designers of such laminated shell structures therefore are forced to employ various approximate methods in conjunction with full-scale laboratory testing. Furthermore, these designers shy away from employment of general unsymmetric lamination of anisotropic layers, which may offer important additional advantages over the more traditional cross-ply and angle-ply constructions toward achievement of a near-optimum design and toward exploitation of the full potential the composite tailoring has to offer. A recent study by Chaudhuri et al.[7] on arbitrarily laminated anisotropic cylindrical shells, based on the CLT and Love-Timoshenko's kinematic relations,[11,12] is an attempt to fill this critical gap. However, the accuracy of the CLT-based solution, presented therein, in the case of thick, laminated shells, needs to be ascertained. The objective of the present study is to derive a closed-form solution of arbitrarily laminated anisotropic cylindrical shells (tubes) of finite length, subjected to axially varying internal pressure, by employing a unified CST-based shell theory. This unified shell theory is an extension of four popular shell theories due to Donnell,[10] Love[11] (Reissner's version[13,14]), Love-Timoshenko[11,12] and Sanders,[15] based on Love-Kirchoff hypothesis, to the CST. Numerical results obtained using this solution will be compared with the available results obtained using the CLT-based closed-form solution of Chaudhuri et al.[7] and the finite-element solution, based on the layerwise constant-shear-angle theory (LCST) of Seide and Chaudhuri.[17,18]

Statement of the Problem

The strain-displacement relations of a circular cylindrical shell (Fig. 1), subjected to axisymmetric loading, are given by[9,19]

$$\epsilon_1 = \epsilon_1^0 + \zeta\kappa_1 \tag{1a}$$

$$\epsilon_2 = \epsilon_2^0 + \zeta\kappa_2 \tag{1b}$$

$$\epsilon_4 = \epsilon_4^0 \tag{1c}$$

$$\epsilon_5 = \epsilon_5^0 \tag{1d}$$

$$\epsilon_6 = \epsilon_6^0 + \zeta\kappa_6 \tag{1e}$$

where, using $\partial/\partial\theta\,(\ldots) = 0$ because of axisymmetry,[9,19]

$$\epsilon_1^0 = u_{0,x} \tag{2a}$$

$$\epsilon_2^0 = w/R \tag{2b}$$

$$\epsilon_4^0 = \phi_\theta - v_0/R \tag{2c}$$

$$\epsilon_5^0 = w_{,x} + \phi_x \tag{2d}$$

$$\epsilon_6^0 = v_{0,x} \tag{2e}$$

$$\kappa_1 = \phi_{x,x} \tag{2f}$$

$$\kappa_2 = 0 \tag{2g}$$

$$\kappa_6 = \phi_{\theta,x} + c_0 v_{0,x}/R \tag{2h}$$

where a comma denotes an ordinary derivative. The x and θ coordinates are equivalent to 1 and 2 coordinates, respectively. The c_0 is a constant that assumes the value of -1, 0, ½, and 1 for extension of kinematic relations, based on Love's first approximation theory (also known as Love-Kirchhoff hypothesis) resulting from Donnell,[10] Love[11] (Reissner's[13,14] version),

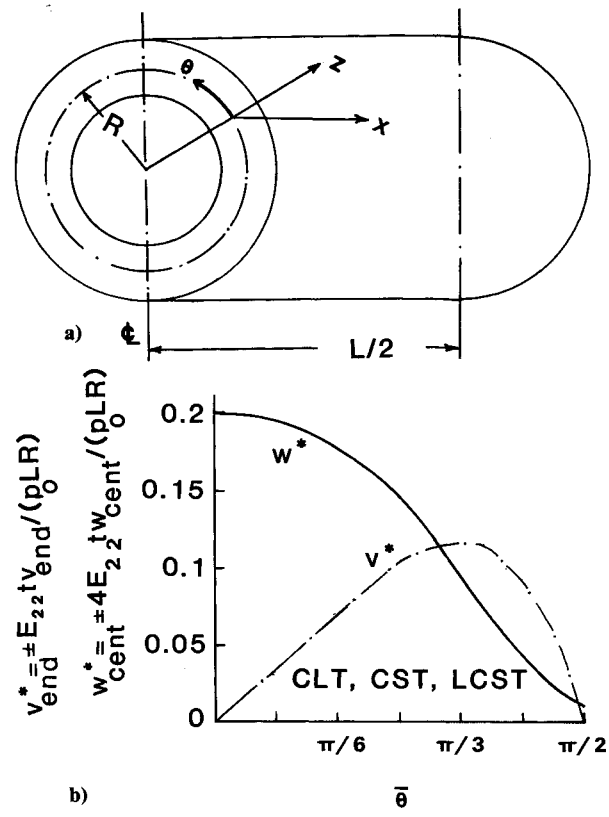

Fig. 1 Cylindrical shells: a) Geometry of the cylindrical shell; b) variation of the central transverse and end circumferential displacements of a two-layer (0 deg/$\bar{\theta}$) cylindrical shell with respect to the fiber orientation of the outer layer.

Sanders,[15] and Love-Timoshenko[12] to the case of FSDT. The equations of equilibrium for a complete circular cylindrical shell (tube) subjected to axially varying internal/external pressure $\pm p(x)$ are given by[9,12,17,19]

$$N_{x,x} = 0 \tag{3a}$$

$$N_{x\theta,x} + Q_\theta/R = 0 \tag{3b}$$

$$N_\theta/R - Q_{x,x} = \pm p(x) \tag{3c}$$

$$M_{x,x} = Q_x \tag{3d}$$

$$M_{x\theta,x} = Q_\theta \tag{3e}$$

$$N_{x\theta} - N_\theta x - c_0 M_{\theta x}/R = 0 \tag{3f}$$

Equation (3a) yields, on integration,

$$N_x = C_1 \tag{4}$$

where C_1 is an integration constant.

The stress resultants, stress couples, and transverse shear forces can be expressed in terms of the reference surface strains and changes of curvature and twist (constitutive relations)[7,9,19,20] through the elastic rigidities, which are as given by Jones.[2] The expression for $N_{x\theta}$ has been chosen such that Eq. (3f) is satisfied.[20]

Derivation of Closed-Form Solution

A closed-form solution to the problem of a pressurized complete cylindrical shell is derived in this section for arbitrary boundary conditions.

Substitution of strain-displacement relations [Eqs. (2)] and the constitutive relations into Eqs. (3) and (4) and then succes-

sive elimination of u_0, v_0, Q_θ, and Q_x from the resulting five coupled ordinary differential equations (O.D.E.) will finally yield a decoupled seventh-order O.D.E. in terms of w. This, on integration, will reduce to a sixth-order O.D.E.:

$$(A_1D^6 + A_2D^4 + A_3D^2 + A_4)w = \pm(A_5D^4 + A_6D^2 + A_7)p(x) + C_2 \tag{5}$$

where the symbolic operator D^n is defined by

$$D^n = \frac{d^n}{dx^n}, \qquad n = 1,\ldots,6 \tag{6}$$

where $A^i = (i = 1,\ldots,7)$ is given by Eqs. (A1), and C_2 is an integration constant. It is noteworthy that, in the case of uniform internal pressure $p(x) = p_0$, the aforementioned seventh-order O.D.E. reduces to a homogenous O.D.E., which implies that the right-hand side of Eq. (5) becomes merely an integration constant C_2^*. It is then evident that the solution due to the uniform pressure is a degenerate case of its counterpart due to axially varying pressure loading, with $C_2^* = \pm A_7p_0 + C_2$. Equation (5), on substitution of

$$A_{16} = A_{26} = A_{45} = B_{11} = B_{22} = B_{12} = B_{66} = D_{16} = D_{26} = 0 \tag{7a}$$

$$A_{45} = 0, \qquad B_{ij} = 0, \qquad i, j = 1, 2, 6 \tag{7b}$$

will reduce to the CST-based governing differential equations (in terms of w) for the special cases of balanced unsymmetric and unbalanced symmetric angle-ply cylindrical shells,[9,19] respectively. Further, Eq. (5), on substitution of

$$A_{16} = A_{26} = A_{45} = B_{16} = B_{26} = D_{16} = D_{26} = 0 \tag{8}$$

will reduce to its counterpart for the case of an unsymmetrically laminated shell of orthotropic construction[8,19] (of which antisymmetric cross ply is a special case), which, on further substitution of

$$B_{11} = B_{22} = B_{12} = B_{66} = 0 \tag{9}$$

will yield the CST-based governing differential equation (in terms of w) for the case of a symmetric cross-ply shell.[8,19] Substitution of $A_{44} = A_{55} \to \infty$ into Eq. (5) will reduce it to its CLT counterpart, which for the case of uniform internal/external pressure p_0 is given by

$$(A_1^*D^4 + A_2^*D^2 + A_3^*)w = \pm A_4^*p_0 + C_2 \tag{10}$$

where A_i^* $(i = 1,\ldots,4)$ are as presented in Chaudhuri et al.,[7,18] with the substitution of $c_0 = 1$ (Love-Timoshenko). Furthermore, substitution of $c_0 = -1$ (Donnell) and Eqs. (7) into Eq. (10) will reduce the latter to those obtained by Reuter[5] for the cases of balanced unsymmetric and unbalanced symmetric angle-ply cylindrical shells, respectively, wherein $A_2^* = 0$. Substitution of $c_0 = 1$ and Eqs. (8) and (9) will reduce Eq. (10) to those obtained by Chaudhuri[21] for the cases of unsymmetric and symmetric thin, laminated shells, respectively, of orthotropic construction.

The w_c, the complementary solution of Eq. (5), is obtained by assuming $w = e^{\lambda x}$, which yields the characteristic equation

$$\lambda^6 + \bar{a}_1\lambda^4 + \bar{a}_2\lambda^2 + \bar{a}_3 = 0 \tag{11}$$

where

$$\bar{a}_i = A_{i+1}/A_i, \qquad i = 1,\ldots,3 \tag{12}$$

Substitution of $\lambda^2 = m$ reduces Eq. (11) to a third-degree polynomial, which can easily be solved,[22] finally yielding

$$w_c = \begin{cases} B_1\sinh(\beta_1x)\sin(\alpha_1x) + B_2\sinh(\beta_1x)\cos(\alpha_1x) \\ \quad + B_3\cosh(\beta_1x)\cos(\alpha_1x) + B_4\cosh(\beta_1x)\sin(\alpha_1x) \\ \quad + B_5\cosh(\gamma_1x) + B_6\sinh(\gamma_1x) \quad \text{if } \bar{Q}_1 > 0 \text{ and } m_1 > 0 \\ B_1\sinh(\beta_1x)\sin(\alpha_1x) + B_2\sinh(\beta_1x)\cos(\alpha_1x) \\ \quad + B_3\cosh(\beta_1x)\cos(\alpha_1x) + B_4\cosh(\beta_1x)\sin(\alpha_1x) \\ \quad + B_5\cos(\gamma_1x) + B_6\sin(\gamma_1x) \quad \text{if } \bar{Q}_1 > \text{ and } m_1 < 0 \\ \sum_{i=1}^{3} f_i(x) \quad \text{if } \bar{Q}_1 < 0 \end{cases} \tag{13}$$

where α_1, β_1, γ_1, m_1, and $\bar{Q}_1$ are as given by Eqs. (A7) and (A8). The B_i $(i = 1,\ldots,6)$ are integration constants, and $f_i(x)$ are defined as

$$f_i(x) = \begin{cases} B_i\cosh(\phi_ix) + B_{i+3}\sinh(\phi_ix) & \text{if } \mu_i > 0 \\ B_i\cos(\phi_ix) + B_{i+3}\sin(\phi_ix) & \text{if } \mu_i < 0 \end{cases} \tag{14}$$

with μ_i $(i = 1, 2, 3)$ being given by Eq. (A9) and $\phi_i = |\mu_i|$.

It may be noted that, for $\bar{Q}_1 = 0$, two of the three real roots of the cubic equation in m are equal, which will yield a degenerate solution for w_c. However, this situation is unlikely to arise in the case of laminated shells under investigation.

The w_p, the particular integral of Eq. (5), can be easily obtained, if $p(x)$ is prescribed. For example, for the case of $p(x) = p_0\cos(\pi x/L)$,

$$w(x) = \frac{\mp p_0[A_5(\pi/L)^4 - A_6(\pi/L)^2 + A_7]\cos(\pi x/L)}{[A_1(\pi/L)^6 - A_2(\pi/L)^4 + A_3(\pi/L)^2 - A_4]} + \frac{C_2}{A_4} \tag{15}$$

In the case of uniform pressure load, $p(x) = \pm p_0$,

$$w_p = (\pm A_7p_0 + C_2)/A_4 \tag{16}$$

Once the complete solution, $w = w_c + w_p$, is known, the remaining unknown quantities Q_x, Q_θ, u_0, and v_0 can easily be obtained, which are as follows:

$$Q_x = (F_1D^5 + F_2D^3 + F_3D)w \tag{17a}$$

$$Q_\theta = (F_4D^5 + F_5D^3 + F_6D)w \tag{17b}$$

$$v_0 = (H_1D^5 + H_2D^3 + H_3D)w + g_{23}\int w\,dx + (g_{26} + g_{25}C_1)x + C_3 \tag{17c}$$

$$u_0 = (H_4D^5 + H_5D^3 + H_6D)w + H_7\int w\,dx + (H_8 + H_9C_1)x + C_4 \tag{17d}$$

where C_3 and C_4 are integration constants, and the constants F_i $(i = 1,\ldots,6)$ and H_i $(i = 1,\ldots,9)$ are as given by Eqs. (A10) and (A11).

The ten integration constants, B_i $(i = 1,\ldots,6)$ and C_i $(i = 1,\ldots,4)$, can be determined by prescribing 5 boundary conditions at each of the 2 ends $(x = \pm L/2)$ of the cylinder. The five boundary conditions are chosen to be one member from each pair of the following equations:

$$(w, Q_x) = (\phi_x, M_x) = (u_0, N_x) = (v_0, N_{x\theta}) = (\phi_\theta, M_{x\theta}) = 0 \tag{18}$$

The commonly used boundary conditions can be described as follows.[7,23]

Simply supported edge $(x = \pm L/2)$:

SS1:

$$w = M_x = N_x = N_{x\theta} = \phi_\theta = 0 \tag{19a}$$

SS2:

$$w = M_x = u_0 = N_{x\theta} = \phi_\theta = 0 \tag{19b}$$

SS3:

$$w = M_x = N_x = v_0 = \phi_\theta = 0 \tag{19c}$$

SS4:

$$w = M_x = u_0 = v_0 = \phi_\theta = 0 \tag{19d}$$

The four clamped-edge conditions CE1, CE2, CE3, and CE4 can be obtained by replacing M_x by ϕ_x in Eqs. (19a–19d), respectively, and the free-edge condition is given by

$$Q_x = M_x = N_x = N_{x\theta} = M_{x\theta} = 0 \tag{20}$$

In the event of loading and boundary conditions being symmetric with respect to the central section of the cylinder,

$$B_2 = B_4 = B_6 = C_3 = C_4 = 0 \tag{21}$$

and the remaining five integration constants can be determined using the prescribed boundary conditions at one end only.

Once the three reference surface displacement components and the two transverse shear force resultants (or the two rotations at the reference surface) are determined, the strains and curvature changes and, finally, the surface parallel stresses can easily be computed. The transverse stresses can be obtained by using Eq. (2.11.1) of Seide.[16]

Numerical Results

The present paper studies, as an example, a two-layer asymmetrically laminated tube of circular cross section, with the fibers in the inner layer oriented in the axial direction of the cylinder, while the $\bar{\theta}$ varies. The layers are of equal thickness. The L, the mean R, and the t of the cylindrical shell are 5080 mm (200 in.), 254 mm (10 in.), and 127 mm (5 in.), respectively. The internal/external pressure $\pm p_0$ is 6895 Pa (100 psi). Analysis of thick-section composite cylinders has assumed increasing importance because of their potential application in the pressure hull of a submarine.[24] Thick section is required to avoid collapse due to buckling under external pressure.

The elastic constants of a unidirectional lamina are assumed to be the same as those used by Spilker et al.[25] The E_{11} and E_{22}, Young's moduli in the directions parallel and transverse to the fibers, are 275.8 GPa (40×10^6 psi) and 6.895 GPa (10^6 psi), respectively. The G_{12} and $G_{13}=G_{23}$, the surface-parallel and transverse shear moduli, respectively, are assumed to be equal to 3.448 GPa (0.5×10^6 psi). The ν_{12}, ν_{13}, and ν_{23} are all assumed to be 0.25. The cylindrical shell is assumed to be simply supported at both ends with SS1-type boundary conditions [see Eq. (19a)]. The CLT- and CST-based numerical results presented below have been obtained using Love-Timoshenko's kinematic relations ($c_0=1$).

Figures 1b–6 show the variation of the transverse displacement and the surface-parallel stresses at the central section of the cylinder (i.e., $x=0$), as well as the surface-parallel displacements at the end ($x=L/2$), with respect to the fiber orientation of the outer layer. The present CST-based closed-form solutions for displacements and stresses are compared with their counterparts, obtained using the CLT-based closed-form solutions of Chaudhuri et al.,[7] as well as the LCST-based finite-element solutions of Seide and Chaudhuri.[17] Details of the formulation and the convergence of the element are available in Refs. 17 and 18 and will not be repeated here. These plots indicate close agreement between the CST and the CLT solutions at a point away from the edge. However, some disagreements between the surface-parallel quantities, computed by the CST and the LCST, are observed for certain fiber orientations of the outer layer (e.g., Figs. 2–6), which bring into action the layerwise variation of the transverse shear deformation. This behavior can be adequately captured by the LCST, to which the CST and the CLT are totally insensitive. It is further noteworthy that the circumferential displacements, as computed by the CLT and CST, do not vary through the thickness, and the layerwise variation of the same, predicted by the LCST, is negligible (Fig. 1b). This is in agreement with what has been observed by Chaudhuri et al.[7] in the case of a corresponding thin, laminated shell. It is also interesting to observe (Fig. 2) that the three theories predict very close end longitudinal displacement at the inner surface of the cylindrical shell. However, the same is not true in the cases of the longitudinal displacements at the outer surface and the interface. The observed differences among the outer surface longitudinal displacement, predicted by the three theories, are maximum in the case of $\bar{\theta}=0$ deg and appear to decrease with the

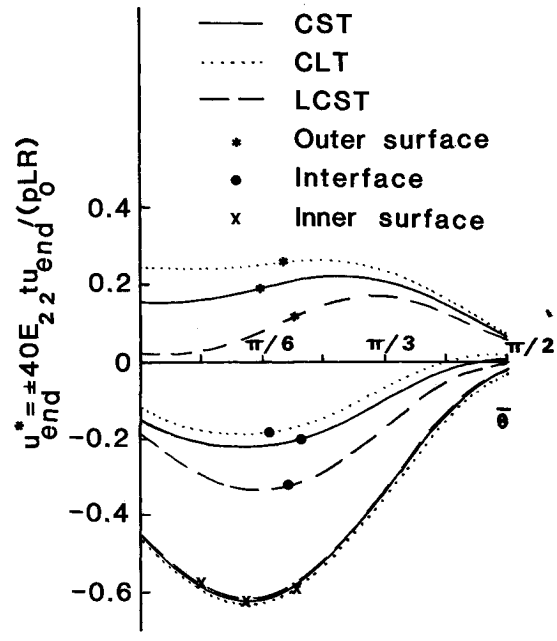

Fig. 2 Variation of the end longitudinal displacement of a two-layer (0 deg/$\bar{\theta}$) cylindrical shell with respect to the fiber orientation of the outer layer.

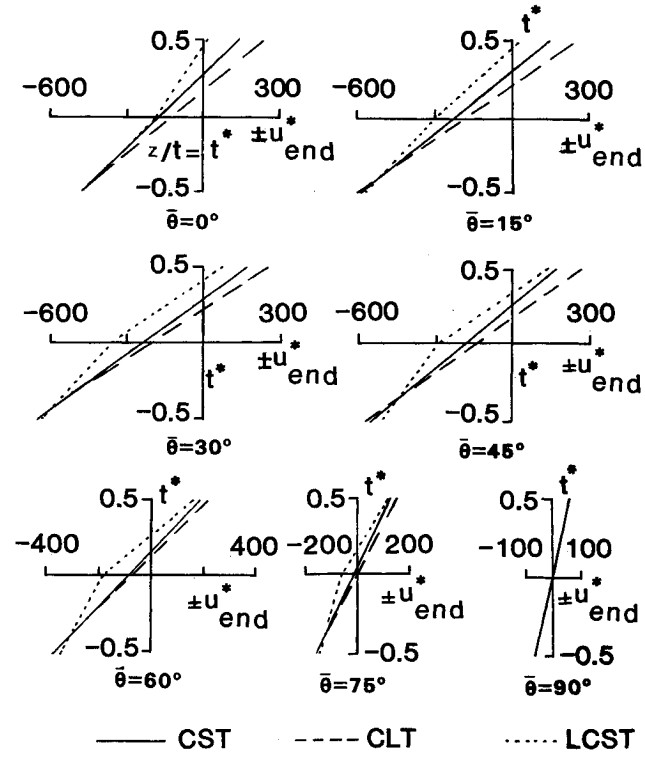

Fig. 3 Variation of the end longitudinal displacement through the thickness of 0 deg/$\bar{\theta}$ cylindrical shells.

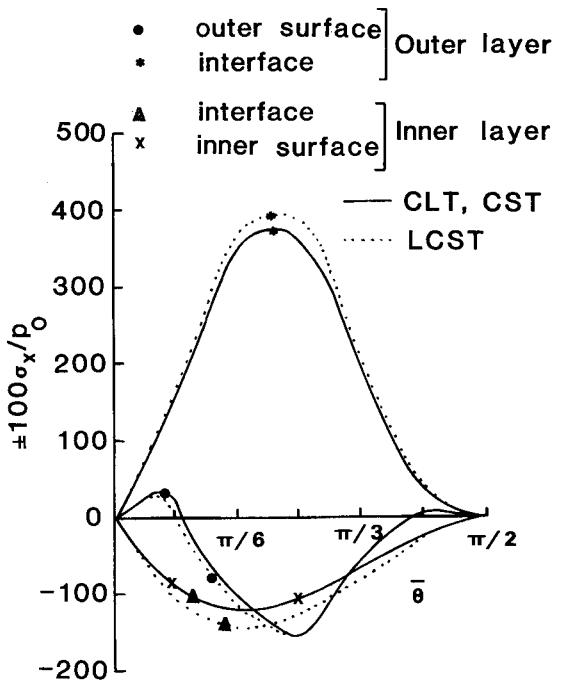

Fig. 4 Variation of the central longitudinal stress of a two-layer (0 deg/$\bar{\theta}$) cylindrical shell with respect to the fiber orientation of the outer layer.

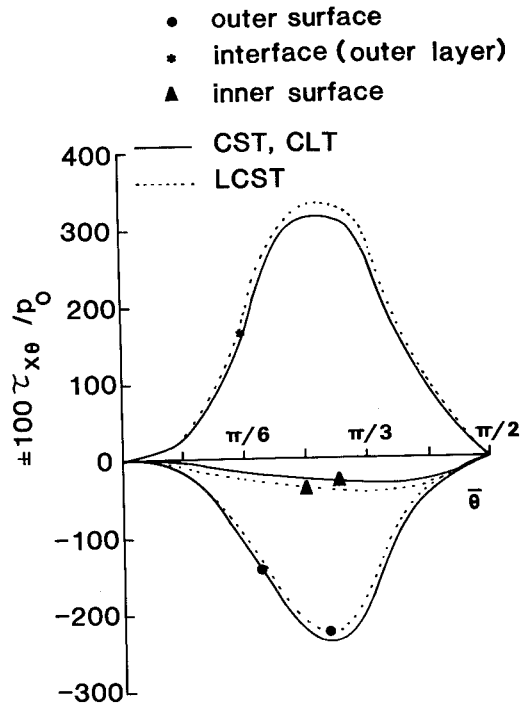

Fig. 6 Variation of the central surface-parallel shear stress of a two-layer (0 deg/$\bar{\theta}$) cylindrical shell with respect to the fiber orientation of the outer layer.

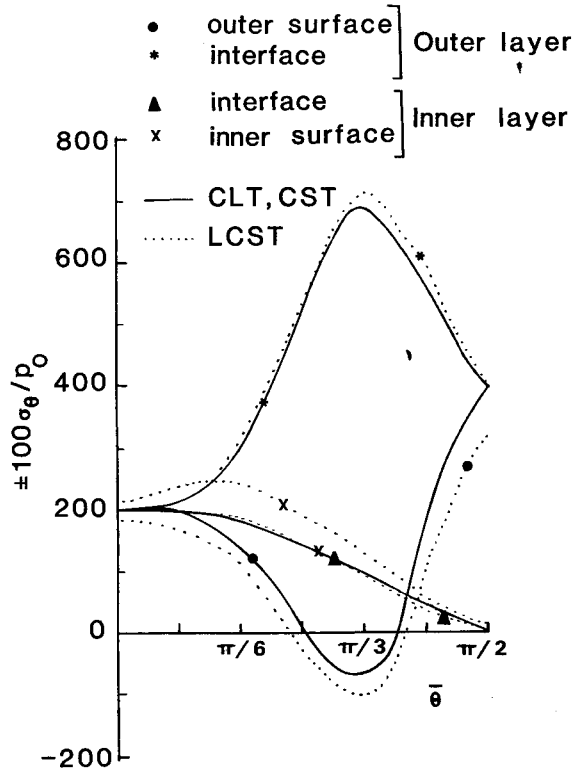

Fig. 5 Variation of the central circumferential stress of a two-layer (0 deg/$\bar{\theta}$) cylindrical shell with respect to the fiber orientation of the outer layer.

increase of the fiber orientation of the outer layer (Fig. 2). However, at the interface, these differences, especially that between the CST and the LCST, first increase as $\bar{\theta}$ increases from 0 deg to 38 deg (approximately) and then decrease with $\bar{\theta}$ increasing to 90 deg (Fig. 2). This behavior is better illustrated in Fig. 3. It may be noted that, in the case of a unidirectional shell ($\bar{\theta}=0$), the LCST predicts smaller rotation of the normal in the outer layer compared with its inner layer. The reverse is true, however, for 15 deg $\leq \bar{\theta} \leq$ 75 deg (approximately). Second, the prediction of the midsurface displacement (membrane effect) is sensitive to the type of the shear-deformation theory employed, except in the case of $\bar{\theta}=90$ deg, which does not exhibit any membrane state (Fig. 3).

It is interesting to observe from Figs. 4–6 that the surface-parallel stresses at the top and the bottom surfaces of the inner (0-deg) layer are almost identical when computed by the CLT and the CST, which implies that these theories can only predict the membrane state in the inner layer. Furthermore, σ_θ and $\tau_{x\theta}$ of the inner layer, as computed by the CLT and the CST, almost coincide with the corresponding inner-layer interface stresses predicted by the LCST, whereas the σ_x of the inner layer, as computed by the first two theories, is very close to the corresponding inner-surface stress predicted by the LCST. In general, the LCST predicts different surface-parallel stresses at the top and bottom surfaces of the inner layer, thus implying the existence of a certain amount of bending stresses in the inner layer, which is essentially a product of the layerwise variation of the transverse shear-deformation effect, to which the CST and the CLT are not sensitive. The difference in behavior of the stresses in the inner and outer layers is, to a small extent, due to the effect of the curvature but is primarily due to such coupling effects as, for example, bending-twisting, produced by the anisotropy of the outer layer (except when $\bar{\theta}=0$ or 90 deg).

Figures 7a and 7b show the axial variation of the displacements w, u, and v in the case of $\bar{\theta}=45$ deg. Axial variation of w is shown in Fig. 7a. The predictions of the CST and the LCST are very close (within 5%), whereas some disagreement is observed between the CST and the CLT predictions. However, this disagreement is not too severe (within 15%), considering the fact that the tube in question is very thick. Axial variation of the circumferential displacement v is also shown in Fig. 7a. The axial variation of the longitudinal displacement component u is shown in Fig. 7b. The interior region of the cylinder is characterized by the membrane state, which is not affected by either the anisotropy of the outer layer or the

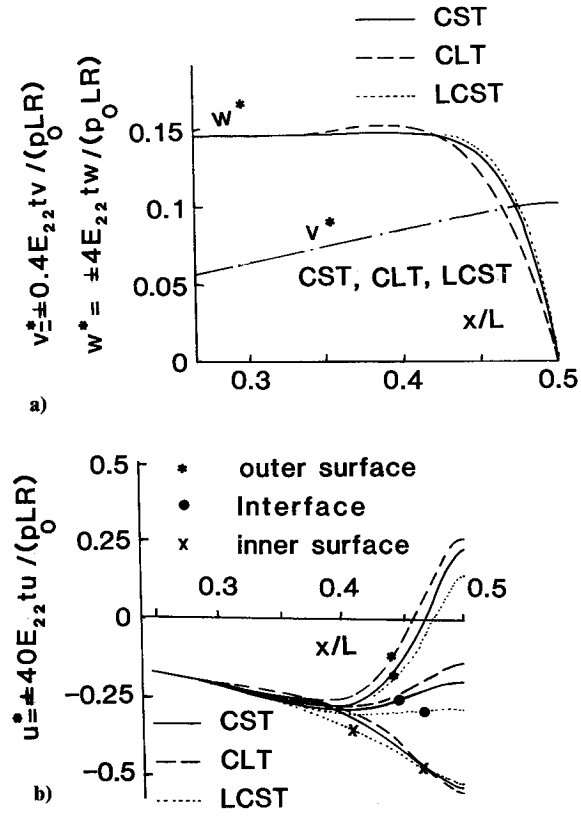

Fig. 7 Axial variation: a) transverse and circumferential; b) longitudinal displacement components of a two-layer (0 deg/45 deg) cylindrical shell.

asymmetry of lamination. In contrast, the end region of the cylinder (approximately one-fifth of the half-length of the cylinder) experiences strong bending action over and above the membrane state. This is what is known as the boundary-layer effect, wherein the bending response brings into action the different transverse shear-deformation effects, approximated by zero, constant, and layerwise constant-shear-angle theories. It is further interesting to note that the end-longitudinal displacements, as predicted by the CLT, the CST, and the LCST, follow definite patterns, with the CST prediction being in between the other two (Fig. 7b).

Figures 8–10 exhibit the variation of the surface-parallel stresses along the axial direction of the cylindrical shell under investigation ($\bar{\theta} = 45$ deg). Most interesting among these plots is Fig. 8b, which exhibits the axial variation of the longitudinal stresses σ_x at the top and the bottom surfaces of the inner layer. As expected, the membrane state is predominant at a section in the central region of the inner layer of the cylinder, wherein the CST and the CLT predictions assume an identical value, which is also close to the inner-surface stress predicted by the LCST. The inner-layer-interface stress in the central region, as predicted by the LCST, is slightly different, which implies the existence of some amount of bending stress, as has been discussed earlier. However, one-fifth to one-quarter of the half-length of the cylinder close to its edge witnesses a very strong boundary-layer effect, which is characterized by the predominant bending response, which, in turn, brings into action the difference transverse shear-deformation effects approximated by zero, constant, and layerwise constant shear-angle theories. In this region, the CLT and the CST predictions can be in error with respect to their LCST counterparts by as much as, if not greater than, 200% and 100%, respectively (Fig. 8b). In comparison, the longitudinal stresses in the outer layer as well as the circumferential stresses and the surface-parallel shear stresses in both the layers experience much less severe boundary-layer effect and the accompanied bending response

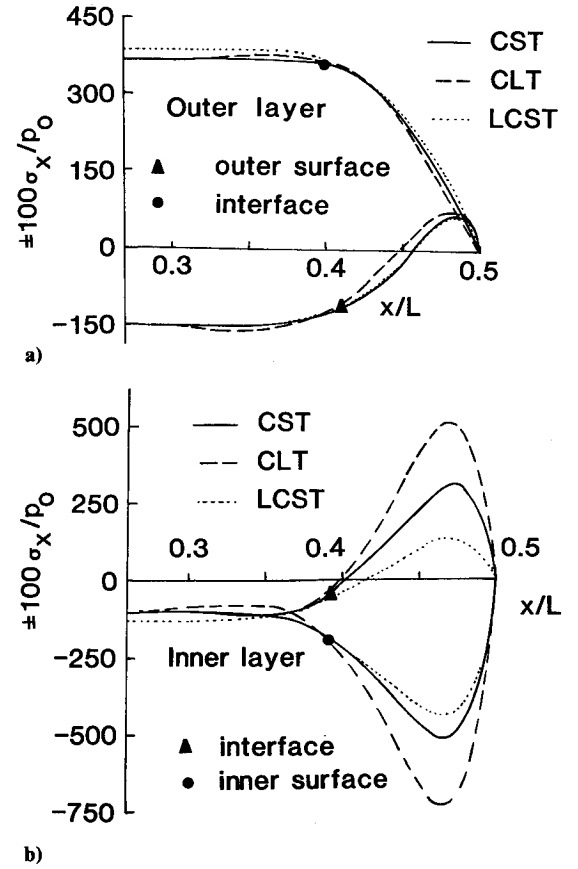

Fig. 8 Axial variation: a) outer layer; b) inner-layer longitudinal stress of a two-layer (0 deg/45 deg) cylindrical shell.

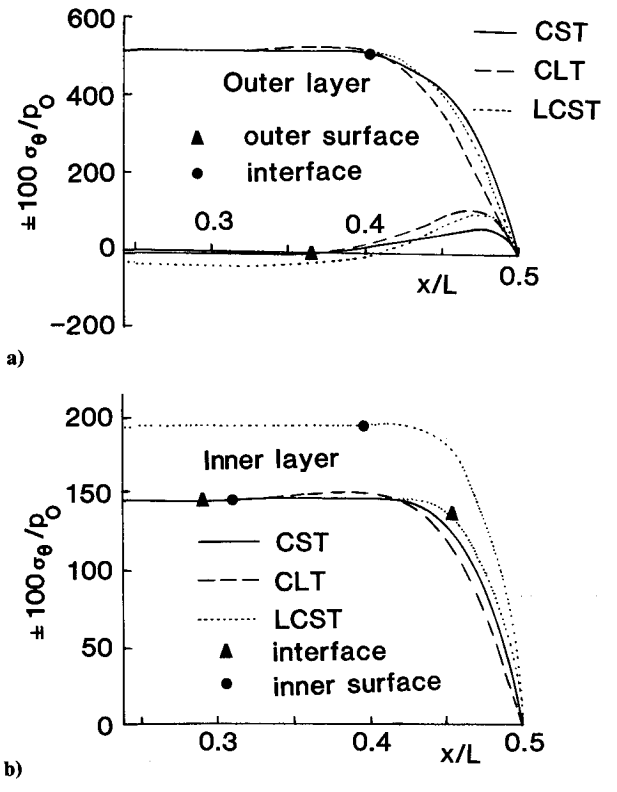

Fig. 9 Axial variation: a) outer layer; b) inner layer circumferential stress of a two-layer (0 deg/45 deg) cylindrical shell.

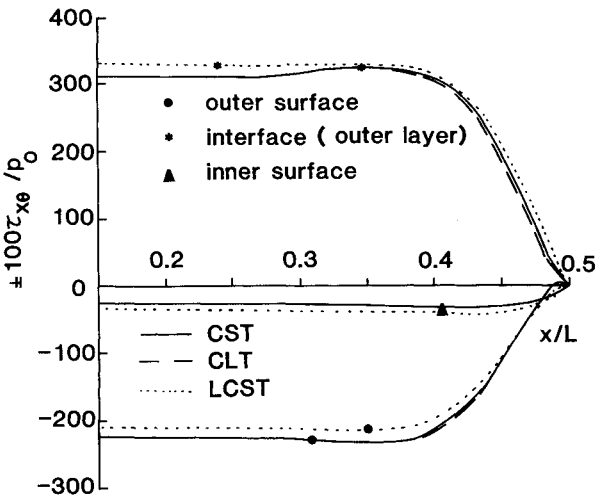

Fig. 10 Axial variation of the surface-parallel shear stress of a two-layer (0 deg/45 deg) cylindrical shell.

in the end region (Figs. 8a–10). It is interesting to observe from Figs. 8a, 9a, and 10 that the outer layer, which witnesses the greater bending response in the central region as a result of anisotropy, experiences the least severe bending action in the end region. Figure 9b demonstrates that, in the central region, the LCST predictions of the inner-layer circumferential stresses are very close to the corresponding inner-layer membrane stresses predicted by the CST and the CLT. In comparison, the LCST predictions of the inner-surface circumferential stresses in the central region are significantly different. This difference, however, gets considerably reduced in the region close to the edge of the cylinder, although the boundary-layer effect and the accompanied bending response still bring into action the different transverse shear-deformation effects aproximated by the CLT, the CST, and the LCST. It may be noted that the preceding CST-based results in general use Eq. (13a), except for $\bar{\theta}=90$ deg, $t\geq 3$ in. and $\bar{\theta}=75$ deg, $t\geq 6$ in. (not shown). In these situations, Eq. (13c) is used.

Summary and Conclusions

Heretofore unavailable closed-form solutions are presented for arbitrarily laminated anisotropic complete cylindrical shells (tubes) under the framework of the CST, also known as the FSDT. These solutions are obtained for shells subjected to axially varying axisymmetric internal/external pressure loading and for arbitrary boundary conditions. A unified CST-based shell theory, which is an extension of Love's first approximation theory (Love-Kirchhoff hypothesis) with the kinematic relations of Donnell, Love-Timoshenko, Love (Reissner's version), and Sanders as special cases, has been employed into the formulation. The previously obtained CST-based solutions for symmetric/unsymmetric cross-ply and balanced-unsymmetric/unbalanced-symmetric angle-ply cylindrical shells under the same loading conditions have been shown to become special cases of the present solution. The available CLT-based solutions can be obtained from the present solutions in the limiting case of the transverse shear rigidities approaching infinity.

The numerical results for two-layer 0 deg/$\bar{\theta}$ tubes with SS1 boundary conditions demonstrate the various coupling effects induced by the asymmetry of lamination and anisotropy of the individual laminae. The key conclusions that emerge from the numerical results can be summarized as follows:

1) The CLT and the CST always predict membrane state of stress in the 0- and 90-deg layers, whereas the LCST predicts the existence of some bending stresses in addition to that. For $\bar{\theta}\neq 0$ deg, 90 deg, bending stresses are predicted by all three theories.

2) The w and v do not exhibit very severe boundary-layer effects, whereas u experiences severe boundary-layer effects and the accompanied bending response, which brings into action the different shear-deformation effects approximated by the CLT, the CST, and the LCST.

3) The longitudinal stress σ_x, which is predicted as the membrane state of stress by the CLT and the CST, in the central region of the 0-deg layer experiences the most severe boundary-layer effect and the accompanied bending response in the end region. The CLT and the CST predictions there can be in error with respect to the LCST by as much as, if not greater than, 200 and 100%, respectively. The $\bar{\theta}$ layer, which, in comparison, witnesses the greater bending response in the central region, experiences far less severe bending action in the end region.

4) Although the LCST, which is essentially a quasi-three-dimensional ply-by-ply analysis, yields the most accurate results, this type of analysis may prove to be prohibitively expensive for a preliminary design of such real-life thick-section composite structures as submarine pressure hulls, consisting of hundreds of layers. The CST, which constitutes an improvement over the CLT without significantly increasing the cost and the complexity of an analysis, then may be recommended for use (with some judgement), because, with the single exception of the inner-surface hoop stress (also, in the limiting case of an exceptionally thick cylinder), the CST-based predictions are either acceptably close or lead to a conservative design.

Solutions presented herein provide important insight into the behavior of arbitrarily laminated thick-section composite cylinders and should facilitate exploitation of composite tailoring in their design.

Appendix

The important constants referred to in the section on derivation of closed-form solution are given below.

The constant coefficients of Eq. (5) are given by

$$A_1 = e_1e_6e_{12} + e_2e_8e_9 + e_4e_{10}e_5 - e_4e_6e_9 - e_2e_5e_{12} - e_1e_8e_{10} \quad \text{(A1a)}$$

$$A_2 = e_1e_6e_{11} - e_1e_{12} + e_6e_{12} - e_2e_8 + e_2e_7e_9 + e_3e_5e_{10} + e_4e_6 + e_4e_9 - e_3e_6e_9 - e_2e_5e_{11} + e_8e_{10} - e_1e_7e_{10} \quad \text{(A1b)}$$

$$A_3 = -e_1e_{11} + e_6e_{11} - e_{12} - e_2e_7 - e_4 + e_3e_6 + e_3e_9 + e_7e_{10} \quad \text{(A1c)}$$

$$A_4 = -e_1e_{11} + e_6e_{11} - e_{12} - e_2e_7 - e_4 + e_3e_6 + e_3e_9 + e_7e_{10} \quad \text{(A1d)}$$

$$A_5 = e_1e_6k_3 + e_2e_9k_2 + e_5e_{10}k_1 - e_6e_9k_1 - e_2e_5k_3 - e_1e_{10}k_2 \quad \text{(A1e)}$$

$$A_6 = (e_6-e_1)e_{15} - (e_2+e_{10})e_{14} + (e_6+e_9)e_{13} \quad \text{(A1f)}$$

$$A_7 = -(e_{13}+e_{15}) \quad \text{(A1g)}$$

wherein

$$e_1 = g_1 + g_3g_{21}, \quad e_2 = g_2 + g_3g_{22}, \quad e_3 = g_4 + g_3g_{23}$$

$$e_4 = g_5 + g_3g_{24}, \quad e_5 = g_{11} + g_{13}g_{21}, \quad e_6 = g_{12} + g_{13}g_{22}$$

$$e_7 = g_{14} + g_{13}g_{23}, \quad e_8 = g_{15} + g_{13}g_{24}, \quad e_9 = g_{16} + g_{18}g_{21}$$

$$e_{10} = g_{17} + g_{18}g_{22}, \quad e_{11} = g_{19} + g_{18}g_{23}, \quad e_{12} = g_{20} + g_{18}g_{24}$$

$$e_{13} = -g_3/g_{10}, \quad e_{14} = -g_{13}/g_{10}, \quad e_{15} = -g_{18}/g_{10} \quad \text{(A2)}$$

with

$$g_1 = b_6 + b_8c_5, \quad g_2 = b_7 + b_8c_4, \quad g_3 = b_4 + b_8c_1$$

$$g_4 = b_{10} + b_8c_2, \quad g_5 = b_{11} + b_8c_3, \quad g_6 = b_{12} + b_{16}$$

$$g_7 = b_{13} + b_{16}c_4, \quad g_8 = b_{14} + b_{16}c_2, \quad g_9 = b_{15} + b_{16}c_3$$

$$g_{10} = b_{17} + b_{16}c_1, \quad g_{11} = b_{19} + B_{11}c_5, \quad g_{12} = b_{20} + B_{11}c_4$$

$$g_{13} = b_{18} + B_{11}c_1, \quad g_{14} = b_{21} + B_{11}c_2$$

$$g_{15} = -D_{11} + B_{11}c_3, \quad g_{16} = b_{24} + B_{16}c_5$$

$$g_{17} = b_{25} + B_{16}c_4, \quad g_{18} = b_{22} + B_{16}c_1$$

$$g_{19} = b_{23} + B_{16}c_2, \quad g_{20} = -D_{16} + B_{16}c_3$$

$$g_{21} = -g_6/g_{10}, \quad g_{22} = -g_7/g_{10}, \quad g_{23} = -g_8/g_{10}$$

$$g_{24} = -g_9/g_{10}, \quad g_{25} = -b_{16}/g_{10}, \quad g_{26} = \pm p/g_{10} \tag{A3}$$

where

$$c_i = -b_i/A_{11} \quad \text{for} \quad i = 1,\ldots,5 \tag{A4}$$

whereas

$$b_1 = A_{16} + (1+c_0)B_{16}/(2R), \quad b_2 = A_{12}/R, \quad b_3 = -B_{11}$$

$$b_4 = B_{11}a_4 + B_{16}a_6, \quad b_5 = B_{11}a_5 + B_{16}a_7$$

$$b_6 = a_2a_7 - b_{11}a_5, \quad b_7 = a_4a_6 - b_{11}a_4, \quad b_8 = A_{16}R + c_0B_{16}$$

$$b_9 = a_1 + (1+c_0)a_2/(2R), \quad b_{10} = A_{26} + c_0B_{26}/R$$

$$b_{11} = -B_{16}R - c_0D_{16}, \quad b_{12} = (B_{12}a_5 + B_{26}a_7)/R$$

$$b_{13} = -1 + (B_{26}a_6 + B_{12}a_4)/R, \quad b_{14} = A_{22}/R^2$$

$$b_{15} = -B_{12}/R, \quad b_{16} = A_{12}/R$$

$$b_{17} = [A_{26} + (1+c_0)B_{26}/(2R)]/R$$

$$b_{18} = B_{16} + (1+c_0)D_{16}/(2R), \quad b_{19} = D_{11}a_5 + D_{16}a_7$$

$$b_{20} = D_{11}a_4 + D_{16}a_6, \quad b_{21} = B_{12}/R$$

$$b_{22} = B_{66} + (1+c_0)D_{66}/(2R), \quad b_{23} = B_{26}/R$$

$$b_{24} = D_{16}a_5 + D_{66}a_7, \quad b_{25} = D_{16}a_4 + D_{66}a_6 \tag{A5}$$

with

$$a_1 = A_{66}R + c_0B_{66}, \quad a_2 = B_{66}R + c_0D_{66}$$

$$a_3 = A_{55}A_{44} - A_{45}^2, \quad a_4 = A_{44}/a_3, \quad a_5 = -A_{45}/a_3$$

$$a_6 = -A_{45}/a_3, \quad a_7 = A_{55}/a_3 \tag{A6}$$

The constants referred to in Eq. (13) are given as follows:

$$m_1 = \bar{A}_1 + \bar{B}_1 - \bar{a}_1/3, \quad m_{2,3} = r_1 \pm is_1$$

where

$$r_1 = -[(\bar{A}_1 + \bar{B}_1)/2 + \bar{a}_1/3], \quad s_1 = (\bar{A}_1 - \bar{B}_1)\sqrt{3}/2$$

with

$$\bar{A}_1 = [-\bar{q}_1/2 + \bar{Q}_1]^{1/3}, \quad \bar{B}_1 = [-\bar{q}_1/2 - \bar{Q}_1]^{1/3}$$

while

$$\bar{p}_1 = -\bar{a}_1^{-2}/3 + \bar{a}_2 \tag{A7a}$$

$$\bar{q}_1 = 2(\bar{a}_1/3)^3 - \bar{a}_1\bar{a}_2/3 + \bar{a}_3 \tag{A7b}$$

$$\bar{Q}_1 = (\bar{p}_1/3)^3 + (\bar{q}_1/2)^2 \tag{A7c}$$

$$\bar{\alpha} = \left[\frac{-r_1 + \sqrt{r_1^2 + s_1^2}}{2}\right]^{1/2}, \tag{A8a}$$

$$\beta_1 = \left[\frac{r_1 + \sqrt{r_1^2 + s_1^2}}{2}\right]^{1/2} \tag{A8b}$$

$$\gamma_1 = \sqrt{|m_1|} \tag{A8c}$$

$$\mu_1 = 2\sqrt{-\bar{p}_1/3}\cos(\bar{\alpha}_1/3), \quad \mu_{2,3} = -2\sqrt{-\bar{p}_1/3}\cos\left(\frac{\bar{\alpha}_1 \pm \pi}{3}\right)$$

where

$$\cos(\bar{\alpha}_1) = \bar{q}_1/(2\sqrt{-(\bar{p}_1/3)^3}) \tag{A9}$$

Finally, the constant coefficients of Eqs. (17) are given by

$$F_1 = -h_{19}/(h_{12} + h_9h_{16})$$

$$F_2 = -(h_{18} + h_{10}h_{16})/(h_{12} + h_9h_{16})$$

$$F_3 = -(h_{15} + h_{11}h_{16})/(h_{12} + h_9h_{16})$$

$$F_4 = F_1(h_5h_9 + h_6), \quad F_5 = F_2(h_5h_9 + h_6) + h_5h_{10} + h_7$$

$$F_6 = F_3(h_5h_9 + h_6) + h_5h_{11} + h_8 \tag{A10}$$

$$H_1 = F_4g_{21} + F_1g_{22}, \quad H_2 = F_5g_{21} + F_2g_{22}$$

$$H_3 = F_6g_{21} + F_3g_{22} + g_{24}, \quad H_4 = c_1H_1 + c_4F_1 + c_5F_4$$

$$H_5 = c_1H_2 + c_4F_2 + c_5F_5, \quad H_6 = c_1H_3 + c_4F_3 + c_5F_6 + c_3$$

$$H_7 = c_1g_{23} + c_2, \quad H_8 = c_1g_{26}, \quad H_9 = c_1g_{25} + 1 \tag{A11}$$

where

$$h_1 = e_2 - e_1e_6/e_5, \quad h_2 = e_1/e_5, \quad h_3 = e_4 - e_1e_8/e_5$$

$$h_4 = e_3 - e_1e_7/e_5, \quad h_5 = e_{10} - e_6e_9/e_5, \quad h_6 = e_9/e_5$$

$$h_7 = e_{12} - e_8e_9/e_5, \quad h_8 = e_{11} - e_7e_9/e_5$$

$$h_9 = -(h_2 + h_6)/(h_1 + h_5), \quad h_{10} = -(h_3 + h_7)/(h_1 + h_5)$$

$$h_{11} = -(h_4 + h_8)/(h_1 + h_5), \quad h_{12} = 1/e_5$$

$$h_{13} = h_2 - e_6/e_5, \quad h_{14} = h_4 - e_8/e_5, \quad h_{15} = -e_7/e_5$$

$$h_{16} = h_{13} + h_1h_9, \quad h_{17} = h_3 + h_1h_{10}$$

$$h_{18} = h_{14} + h_1h_{11} \tag{A12}$$

References

[1]Judge, J. F., "Composite Material: The Coming Revolution," *Airline Management and Marketing,* Sept. 1969, pp. 85–91.

[2]Jones, R. M., *Mechanics of Composite Materials,* McGraw-Hill, New York, 1975.

[3]Ambartsumyan, S. A., "Calculation of Laminated Anisotropic Shells," *Izvestiya Akademii Nauk Armyanskoi SSR, Fiziko-Matematicheskie Estestvennye i Tekhnichskie Nauk,* Vol. 16, No. 3, 1953, p. 15.

[4]Dong, S. G., Pister, K. S., and Taylor, R. L., "On the Theory of Laminated Anisotropic Shells and Plates," *Journal of Aerospace Sciences,* Vol. 29, 1962, pp. 969–975.

[5]Reuter, R. C., "Analysis of Shells Under Internal Pressure," *Journal of Composite Materials,* Vol. 6, Jan. 1972, pp. 94–113.

[6]Bert, C. W. and Reddy, V. S., "Cylindrical Shells of Bimodulus Material," *Journal of Engineering Mechanics Division,* ASCE, Vol. 108, May 1982, pp. 657–688.

[7]Chaudhuri, R. A., Bataraman, K., and Kunukkasseril, V. X., "Arbitrarily Laminated Anisotropic Cylindrical Shell Under Internal Pressure," *AIAA Journal*, Vol. 24, Nov. 1986, pp. 1851–1858.

[8]Abu-Arja, K. R. and Chaudhuri, R. A., "Influence of Transverse Shear Deformation on Scaling of Cross-Ply Cylindrical Shells," *Journal of Composite Materials* (to be published).

[9]Abu-Arja, K. R. and Chaudhuri, R. A., "Moderately Thick Angle-Ply Cylindrical Shells Under Internal Pressure," *Journal of Applied Mechanics* (to be published).

[10]Donnell, L. H., *Stability of Thin Walled Tubes in Torsion*, NACA Rept. 479, 1933.

[11]Love, A. E. H., *A Treatise on the Mathematical Theory of Elasticity*, 4th ed., Dover, New York, 1944.

[12]Timoshenko, S. P. and Woinowsky-Krieger, S., *Theory of Plates and Shells*, 2nd ed., McGraw-Hill, New York, 1959.

[13]Reissner, E., "A New Derivation of the Equations for the Deformation of Elastic Shells," *American Journal of Mathematics*, Vol. 63, 1941, pp. 177–184.

[14]Kraus, H., *Thin Elastic Shells*, Wiley, New York, 1967.

[15]Sanders, J. L., "An Improved First-Approximation Theory for Thin Shells," NASA R-24, 1959.

[16]Seide, P., *Small Elastic Deformation of Thin Shells*, Noordhoff International, Leiden, The Netherlands, 1975.

[17]Seide, P. and Chaudhuri, R. A., "Triangular Finite Element for Analysis of Thick Laminated Shells," *International Journal for Numerical Methods in Engineering*, Vol. 24, 1987, pp. 1563–1579.

[18]Chaudhuri, R. A., "Static Analysis of Fiber Reinforced Laminated Plates and Shells with Shear Deformation Using Quadratic Triangular Elements," Ph.D. Dissertation, Dept. of Civil Engineering, Univ. of Southern California, Los Angeles, CA, 1983.

[19]Abu-Arja, K. R., "Static Analysis of Laminated Fiber Reinforced Plates and Shells with Shear Deformation," Ph.D. Dissertation, Department of Civil Engineering, Univ. of Utah, Salt Lake City, UT, 1986.

[20]Kunukkasseril, V. X., "Free Vibration of Multi-Layered Anisotropic Cylindrical Shells," Rept. WVT-6717, AD-649662, Watervliet Arsenal, Watervliet, NY, 1967.

[21]Chaudhuri, R. A., "Structural Behavior of FRP Rectangular Plates and Cylindrical Shells," M.S. Thesis, Dept. of Aeronautical Engineering, Indian Institute of Technology, Madras, India, March 1974.

[22]Korn, G. A. and Korn, T. M., *Mathematical Handbook for Scientists and Engineers*, 2nd ed., McGraw-Hill, New York, 1968.

[23]Hoff, N. J. and Rehfield, L. W., "Buckling of Axially Compressed Circular Cylindrical Shells at Stresses Smaller Than the Classical Critical Value," *Journal of Applied Mechanics*, Vol. 32, Sept. 1965, pp. 542–546.

[24]Garala, H. J., "Experimental Evaluation of Graphite-Epoxy Composite Cylinders Subjected to External Hydrostatic Compressive Loading," *Proceedings of the 1987 SEM Spring Conference on Experimental Mechanics*, Society for Experimental Mechanics, Bethal, CT, 1987, pp. 948–951.

[25]Spilker, R. L., Chou, S. C., and Orringer, O., "Alternate Hybrid-Stress Elements for Analysis of Multi-Layer Composite Plates," *Journal of Composite Materials*, Vol. 11, Jan. 1977, pp. 51–70.